JOURNAL OF MATERIALS SCIENCE 30 (1995) 2348–2351

Crystal growth of Bi–Sr–Ca–Cu–O from Sr–Ca–Cu–O thin films

R. KAIGAWA, T. SAKAGUCHI, R. HERRMANN, C. KAITO, H. MIKI,* Y. NAKAYAMA
*Department of Physics, and *Department of Electrical and Electronic Engineering, Ritsumeikan University, Kita-ku Kyoto 603-77, Japan*

Bi–Sr–Ca–Cu–O crystals have been prepared from amorphous Sr–Ca–Cu–O thin films by annealing at 890 °C in the presence of bismuth oxide vapour. $Sr_{0.8}Ca_{0.2}CuO_2$ (08021) and $Bi_2(Sr, Ca)_2CuO_6$ (2201) crystals initially appeared. On further annealing, needle crystals of $Sr_{14-x}Ca_xCu_{24}O_{41}$ $(14 - x)$ grew. These $14 - x$ needle crystals gradually changed to 2201 needle crystals, which further changed to crystals of the nominal composition Bi–Sr–Ca–Cu–O with a *c*-axis length of 1.69 nm.

1. Introduction

The high-temperature superconductors of the Bi–Sr–Ca–Cu–O [1] system have a specific property in which the critical temperature is changed by a controllable number of layers of the copper oxide. This series of compounds is conveniently described as the homologous series of $Bi_2Sr_2Ca_{n-1}Cu_nO_{2n+4}$. The lengths of the *c*-axes differ according to the CuO_2 layer number, *n*: $c \simeq 2.45$ nm ($n = 1$), $c \simeq 3.06$ nm ($n = 2$), $c \simeq 3.70$ nm ($n = 3$), and $c \simeq 4.30$ nm ($n = 4$) [2]. The structures are described on the basis of stacking layers, BiO, SrO, CaO, and CuO_2. Recently Kishida *et al.* [3] found a crystal with a *c*-axis of 3.9 nm by the self-flux method, which cannot be presented as belonging to the homologous series.

On heat treatment in air, a certain amount of the bismuth oxide in the Bi–Sr–Ca–Cu–O crystals vaporizes, and the deficiency of the bismuth oxide results in the formation of by-products, for example Sr–Ca–Cu–O crystals [4, 5]. Shimoyama *et al.* [6] have recently found that the growth of the Sr–Ca–Cu–O was decreased by controlling the bismuth oxide vapour pressure. This suggests that the formation of the Sr–Ca–Cu–O crystals in the Bi–Sr–Ca–Cu–O phase is sensitive to the bismuth oxide vapour pressure. Hence, it is worth investigating the reaction between bismuth oxide and the Sr–Ca–Cu–O phase, especially, as from the application point of view, the growth of superconducting thin films is an important subject.

In the present work, the growth process of Bi–Sr–Ca–Cu–O crystals and Sr–Ca–Cu–O crystals from amorphous Sr–Ca–Cu–O films, by annealing them in the presence of the bismuth oxide vapour, has been investigated. A new structure with a *c*-axis of 16.9 nm has been found.

2. Experimental procedure

Thin films of Sr–Ca–Cu–O (Sr:Ca:Cu $\simeq$ 2:2:3) were prepared on MgO (1 0 0) substrates ($10 \times 10 \times 0.5$ mm^3) at room temperature by co-evaporation using a molecular beam epitaxy (MBE) evaporator. The evaporation chamber was evacuated by a cryopump, to a base pressure of about 1×10^{-9} torr (1 torr = 133.322 Pa). The molecular beams of strontium, calcium and copper were obtained from their respective metallic sources, by means of three Knudsen cells. Molecular beam intensities were monitored with an ionization nude gauge near the substrate. The gauge was kept away from the substrate during evaporation. To prepare the starting film, oxygen was dosed to the substrate through a stainless steel tube during the evaporation. The chamber pressure increased to about 1×10^{-5} torr. In order to activate the oxygen gas, it was irradiated by ultraviolet light. The thickness of the as-deposited films was about 500 nm. The deposition rate was about 25 nm min^{-1}. In order to add the bismuth and the oxygen to the film, the sample mounted on $Bi_2Al_4O_9$ was housed in an alumina crucible with a cover, and annealed at 890 °C in air. The Bi–Sr–Ca–Cu–O partially melts at 890 °C. The $Bi_2Al_4O_9$ substrate was synthesized from mixed powders of Bi_2O_3 and Al_2O_3 by annealing at 850 °C for 2 h in an alumina crucible in air.

The composition of the film was determined by X-ray fluorescence analysis with the aid of synthesized standard samples. The crystal structure of the annealed thin films was analysed by X-ray diffraction (XRD) using CuK_α radiation. The electrical resistances were measured by the standard four-probe method using silver-evaporated electrodes. Analyses of morphology and composition of the grown crystals were performed using a JSM 6400 scanning electron microscope (SEM) interfaced to an energy-dispersive X-ray spectroscopy (EDS) analysis system.

3. Results and discussion

The ratio of bismuth to copper contents in the films annealed by the present method was analysed by

0022–2461

X-ray fluorescence analysis, as shown in Fig. 1. The bismuth content in the film linearly increased with increasing annealing times.

The structure of the unannealed film was amorphous, because the XRD pattern showed a halo. By annealing the film for 0.5 h, three phases of $Sr_{0.8}Ca_{0.2}CuO_2$ (08021), Bi–(Sr, Ca)–O, which is an another by-product of the bismuth-based superconductor, and $Bi_2(Sr, Ca)_2CuO_6$ (2201) appeared, as shown in Fig. 2a. The *b*-axis of the 08021 phase is predominantly perpendicular to the substrate surface, because (0 *k* 0) peaks of the 08021 phase are predominantly observed, and the *c*-axis of the 2201 phase is perpendicular to the substrate surface. A *b*-axis length of 1.625 nm of the 08021 phase was determined from the value of the (0 1 2 0) diffraction line. The 08021 composition was determined from this *b*-axis length [7]. The temperature dependence of the resistance of this sample given in Fig. 3a, shows a semiconductive

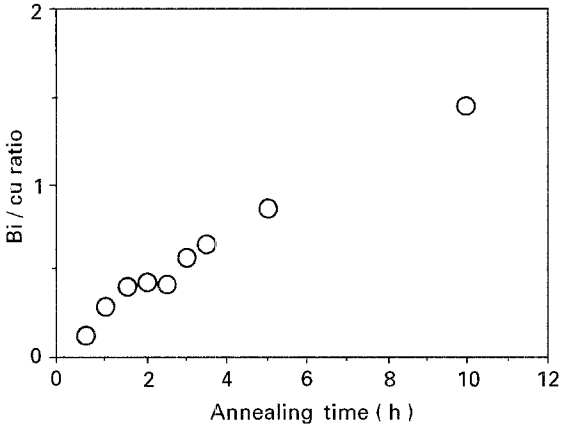

Figure 1 Ratio of bismuth to copper contents in the films as a function of the annealing time.

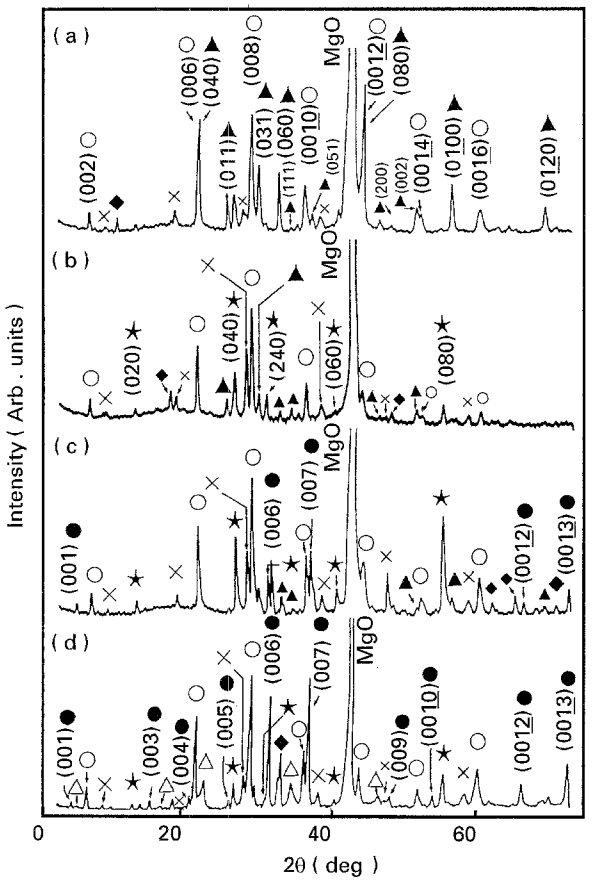

Figure 2 The XRD patterns of the films annealed at 890 °C for (a) 0.5 h, (b) 1 h, (c) 2.5 h and (d) 10 h. (○) 2201 phase, (▲) 08021 phase, (★) 14-*x* phase, (×) Bi–(Sr, Ca)–O, (●) the new phase, (△) 2212 phase, (◆) the unidentified peak.

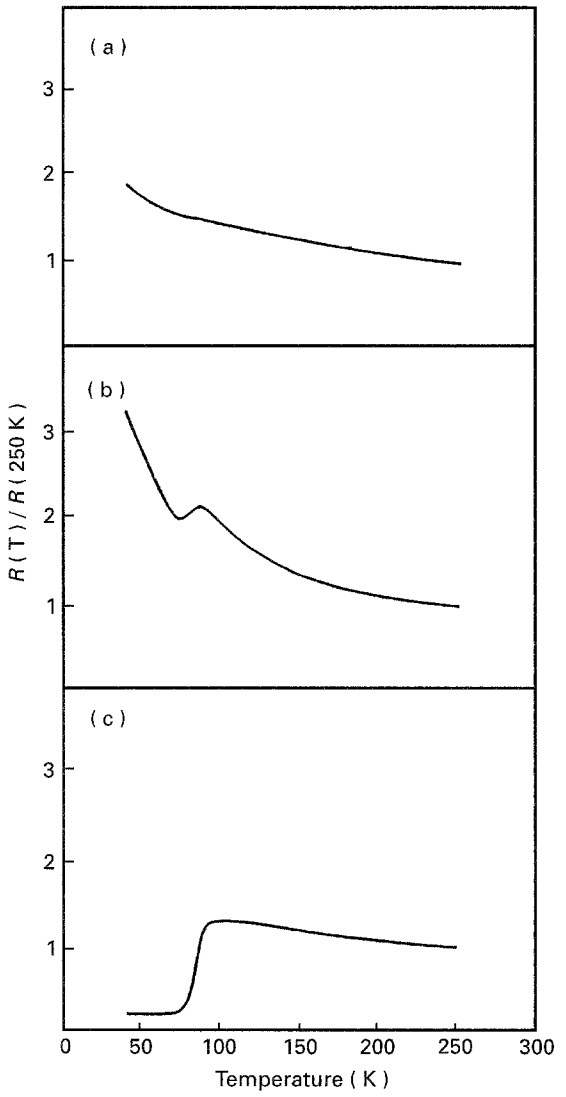

Figure 3 Temperature dependence of the resistance (normalized at 250 K) of the films annealed at 890 °C for (a) 0.5 h, (b) 2.5 h, and (c) 10.0 h.

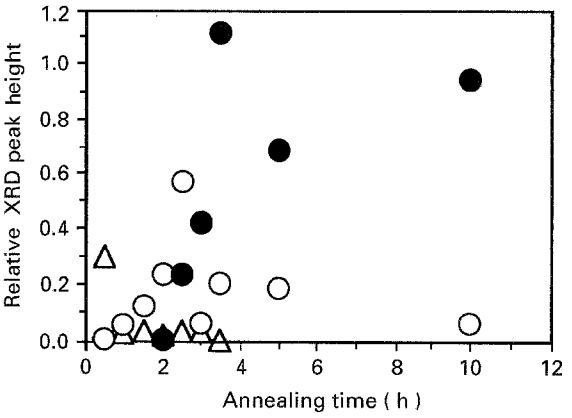

Figure 4 The relative XRD peak height of (△) $(0\,6\,0)_{08021}$, (○) $(0\,8\,0)_{14-x}$ and (●) $(0\,0\,7)_{new\ phase}$ normalized to the $(0\,0\,8)_{2201}$ as a function of the annealing time.

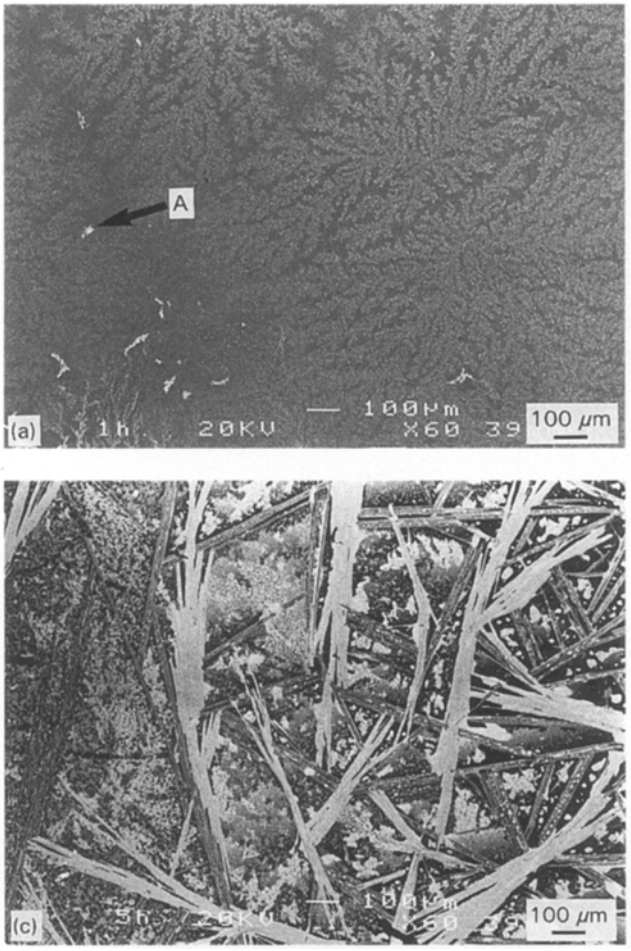

Figure 5 Back-scattered electron images of the surface of the films annealed at 890 °C for (a) 1 h, (b) 2 h, and (c) 5 h.

behaviour due to the 2201 phase. On annealing for more than 1 h, the XRD peak of the 08021 phase gradually disappeared; however, a $Sr_{14-x}Ca_xCu_{24}O_{41}$ [4] ($14-x$) phase, whose *b*-axis was perpendicular to the substrate surface, appeared in addition to the 2201 phase as shown in Fig. 2b.

Fig. 3b shows the temperature dependence of resistance of the film annealed for 2.5 h. A transition, suggesting a superconducting behaviour, is observed at about 85 K. In the XRD pattern for this sample, in addition to the peaks of the above two phases, a new series of the peaks at $2\theta = 5.25°$, 31.75°, 37.20°, 66.25°, and 72.65° were observed as shown in Fig. 2c. When we determine that the peak at $2\theta = 5.25°$ corresponds to (0 0 1), these peaks are considered to correspond to the (0 0 *l*) series of a unit cell where the length of the long axis is 1.69 nm. This phase can also be seen in the sample annealed for 10 h, as shown in Fig. 2d. The length of the *c*-axis of the new phase does not correspond to the homologous series. This is similar to the growth of the single crystal with a *c* axis of 3.9 nm [3].

The ratios of the peak height of $(0\,6\,0)_{08021}$ to $(0\,0\,8)_{2201}$, $(0\,8\,0)_{14-x}$ to $(0\,0\,8)_{2201}$, and $(0\,0\,7)_{\text{new phase}}$ to $(0\,0\,8)_{2201}$ were plotted as a function of the annealing time in Fig. 4. From the figure one can roughly estimate the change of the amount of the 08021 phase, the $14-x$ phase and the new phase, relative to the 2201 phase. At first the 08021 phase appeared, but soon it almost disappeared. The amount of the $14-x$ phase increased with a logarithmic relation until the annealing time at 2.5 h, after that, it decreased with increasing annealing time. When the amount of the $14-x$ phase reached a maximum (at 2.5 h), a new phase of $c = 16.9$ nm appeared, and this new phase increased with the decrease of the $14-x$ phase. Because the bismuth in the film increases with the increasing annealing time and the $14-x$ phase reacts with bismuth, it seems that a certain amount of the $14-x$ crystal changes into the 2201 phase and/or the new phase.

Typical back-scattered SEM images are shown in Fig. 5. The EDS analysis shows that the bright parts in Fig. 5 suggest the existence of bismuth atoms. On annealing the film for 1.0 h, the 2201 phase grows like a dendrite on the matrix of the 08021 phase, as shown in Fig. 5a. (When the amorphous Sr–Ca–Cu–O film was annealed in the absence *of the bismuth oxide vapour, only the* 08021 *phase grew.*) *In the figure, the Bi*–(Sr, Ca)–O phase (indicated by arrow A) is also observed. On further annealing, the needle crystals of the $14-x$ phase apparently grow, as shown in Fig. 5b. All the crystals above were identified by EDS analysis. In the SEM images shown in Fig. 6a, the large needle crystal (indicated by A) was the $14-x$ phase, the small rectangular crystals (indicated by B) were the 08021 phase, and the flake crystals (indicated by C) were the 2201 phase. The flake shape is a typical one for the Bi–Sr–Ca–Cu–O crystal. Even if the sample was annealed further, the 2201 phase which grew in the flake shape, remained in the film. However, the $14-x$ needle crystals gradually changed to the Bi–Sr–Ca–Cu–O phase keeping nearly the same morphology of $14-x$ phase needle crystal. The contrast of the back-scattering electron image in Fig. 5c suggests this. The needle crystals of the 2201 phase with smooth surface further changed to crystals containing many steps whilst retaining the needle shape. Fig. 6b and c show these processes of the transformation of each crystal: the $14-x$ phase (indicated by D) → the 2201 phase (indicated by E) → the crystal containing many steps (indicated by F). The composition of crystal F differs from the 2201 phase. The EDS intensity analysis implies that the composition of the crystal containing many steps may be presented as $Bi_{2.96}Sr_{2.36}Ca_{0.50}Cu_{2.00}O_y$ on average. It is evident that the crystal F is the new phase because, from the

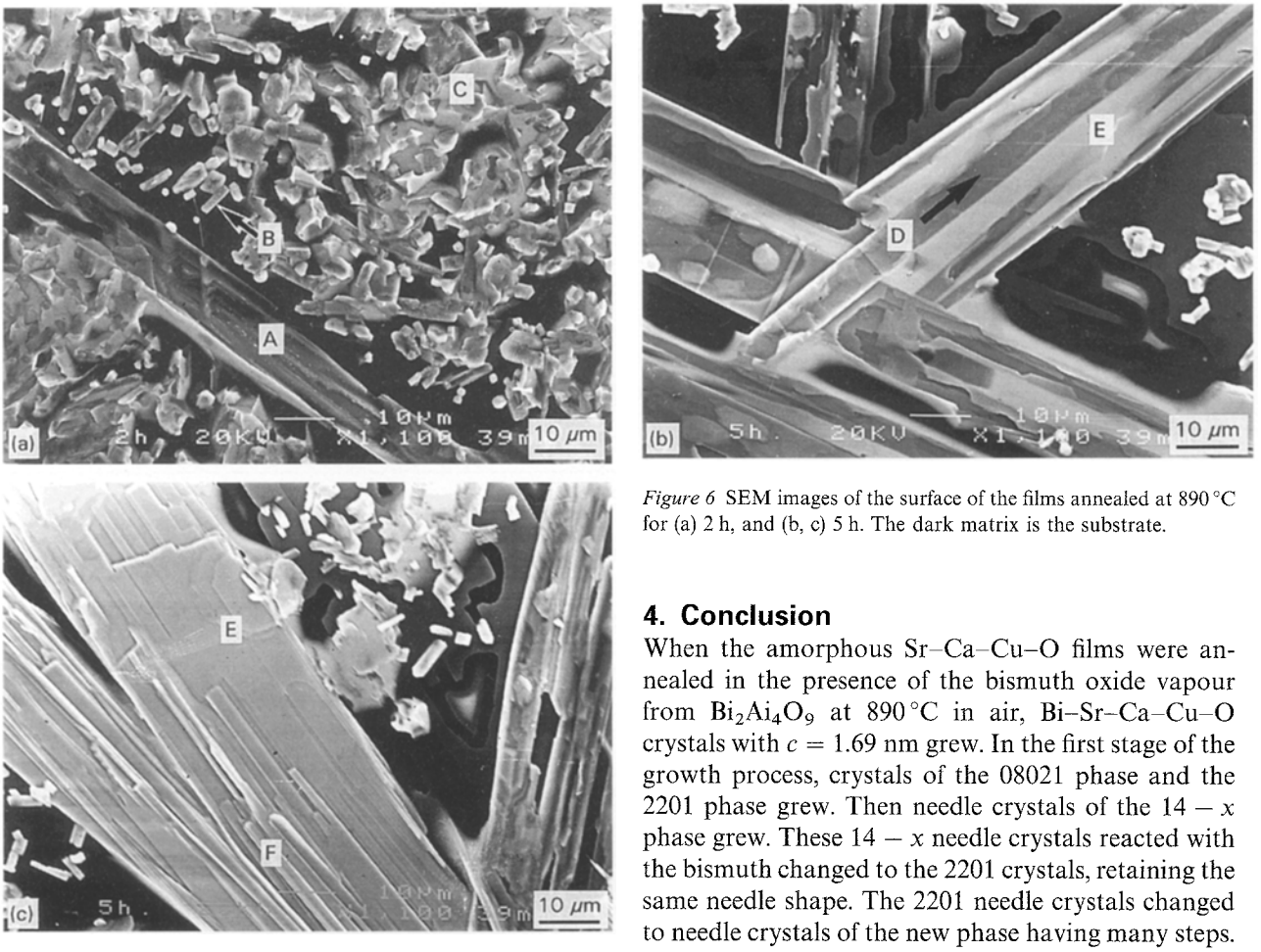

Figure 6 SEM images of the surface of the films annealed at 890 °C for (a) 2 h, and (b, c) 5 h. The dark matrix is the substrate.

XRD analysis, there are no other crystals close to this composition, and crystal F grows more and more with increasing annealing time after 2.5 h. It could be concluded that the new phase resulted from the 2201 crystal whilst retaining the needle shape of the $14 - x$ phase. The details of the crystal structure analysis of this phase will be published elsewhere.

From the XRD measurement, the $Bi_2Sr_2CaCu_2O_8$ (2212) phase was not seen in the four samples annealed between 2.5 and 5 h. However, from the resistance measurements for these samples, transitions at 85 K were observed. In addition, it was found that the transition step increases with increase of the peak height of the new phase. This suggests that these transitions may be due to the new phase; however, it seems also possible that the transitions are due to a small volume fraction of 2212 phase which was not detected by the XRD measurements, because a small amount of the 2212 phase appeared in the film annealed for 10 h, as shown in Fig. 2d. The superconducting characteristic of the new phase and a detailed crystal structure must be determined from the single-crystal film of the new phase.

4. Conclusion

When the amorphous Sr–Ca–Cu–O films were annealed in the presence of the bismuth oxide vapour from $Bi_2Ai_4O_9$ at 890 °C in air, Bi–Sr–Ca–Cu–O crystals with $c = 1.69$ nm grew. In the first stage of the growth process, crystals of the 08021 phase and the 2201 phase grew. Then needle crystals of the $14 - x$ phase grew. These $14 - x$ needle crystals reacted with the bismuth changed to the 2201 crystals, retaining the same needle shape. The 2201 needle crystals changed to needle crystals of the new phase having many steps. The crystals of the new phase grew only from the needle crystals of the $14 - x$ phase.

References

1. H. MAEDA, Y. TANAKA, M. FUKUTOMI and T. ASANO, *Jpn J. Appl. Phys.* **27** (1988) L209.
2. K. K. FUNG, C. Y. YANG and Y. F. YAN, *Appl. Phys. Lett.* **55** (1989) 280.
3. S. KISHIDA, H. TOKUTAKA, M. KATAYAMA, K. NISHIMORI, N. ISHIHARA and T. YUMOTO, *Jpn J. Appl. Phys.* **32** (1993) L398.
4. E. M. McCARRON III, M. A. SUBRAMANIAN, J. C. CALABRESE and R. L. HARLOW, *Mater. Res. Bull.* **23** (1988) 1355.
5. J. SHIMOYAMA, J. KASE, S. KONDOH, T. MATSUBARA and T. MORIMOTO, "Electronic Properties and Mechanisms of High T_c Superconductors" (Elsevier Science, North Holland, 1992).
6. J. SHIMOYAMA, N. TOMITA, T. MORIMOTO, H. KITAGUCHI, H. KUMAKURA, K. TOGANO, H. MAEDA, K. NOMURA and M. SEIDO, *Jpn J. Appl. Phys.* **31** (1992) L1328.
7. M. T. GAMBARDELLA, B. DOMENGES and B. RAVEAU, *Mater. Res. Bull.* **27** (1992) 629.

Received 31 January
and accepted 27 September 1994